Cement & Concrete Composites 39 (2013) 104–114

Contents lists available at SciVerse ScienceDirect

Cement & Concrete Composites

journal homepage: www.elsevier.com/locate/cemconcomp

Reactivated cementitious materials from hydrated cement paste wastes

Ricardo Serpell, Mauricio Lopez *

Department of Construction Engineering and Management, School of Engineering, Pontificia Universidad Catolica de Chile, Santiago, Chile

ARTICLE INFO

Article history:
Received 31 May 2011
Received in revised form 22 March 2013
Accepted 24 March 2013
Available online 4 April 2013

Keywords:
Thermal treatment
Compressive strength
Cement paste
Cement recycling
Recycled concrete
Waste management

ABSTRACT

Hydrated cement pastes subjected to high temperature dehydration have been shown to develop a cementitious behavior upon rehydration that could enable recycling of hydrated cement wastes as alternative binders of high environmental value. In order to evaluate the potential of this recycling option it is first necessary to identify material and process factors affecting the performance of the reactivated cementitious materials produced. This paper presents the findings of a fractional factorial experiment designed to screen factors based on their effect on the strength developed by pastes incorporating materials reactivated from laboratory sourced hydrated cement pastes. Results allowed identification of factor and factor-interaction effects involving 7 of the 9 factors under study, which would be relevant in optimizing the recycling process. Highest strengths observed in the experimental region explored were 20, 32.8 and 39 MPa at 7, 28, and 90 days, respectively, for reactivated material pastes mixed at 0.7 W/CM ratio.

1. Introduction

The cement and concrete industry faces an ever increasing demand to reduce its impact on the environment. Concrete is nowadays one of the most used manufactured materials, with worldwide production currently exceeding 20,000 million tons per year, as estimated from the 2.9 billion tons of Portland cement produced in 2009 [1]. Therefore, small changes in concrete technology have the potential to produce a significant change to the environmental footprint of the industry. Three main sources of impact can be identified: the consumption of natural resources and energy to produce both Portland cement and concrete, the greenhouse gas emissions due mostly to the production of Portland cement [2–5], and the large contribution of concrete to the construction and demolition solid wastes [3]. Recycling cement and concrete wastes can reduce the impact derived from these sources, and, adding to the environmental benefit of a sound material cycle, this substitution can be economically viable due to the savings in energy and transportation that could be achieved [6].

Major concrete components must be processed separately in order to source recycled materials for the production of new mixtures. In the case of aggregates, substitution of natural materials by recycled concrete aggregates (RCAs) can reach 100% by adjusting mixing methods to RCA properties [7,8]. Quality RCA have to be freed from hydrated cement paste residues which would otherwise limit the performance of the new concrete [9]. When an aggregate improvement process involving heating and grinding is used, 75% of the original wastes can be recovered as high quality fine and coarse RCA, leaving 25% of fine concrete powder waste comprised mostly of hydrated cement paste (HCP) [10]. These fines, however, are normally discarded or used in low value applications, despite being the by-product of the higher costing component of the original concrete both in economic and in environmental terms.

Recycling of HCP wastes as binders for the production of new concretes holds high environmental value for the cement and concrete industry. Impact from natural resources consumption and waste generation would be further reduced, and, depending on the technical characteristics of the recycling process developed, greenhouse gas emissions and energy consumption could also be reduced, as recycled materials partially substitute Portland cement.

Potential paths to recycling of HCP wastes identified in recent publications range from the production of Controlled Low Strength Materials using fines from crushed concrete together with supplementary cementitious materials (SCMs) [11,12], to the production of clinkers using concrete wastes as raw-feed [13,14]. Somewhat in between the range above, a promising alternative is the reactivation of the cementitious properties of the HCP wastes by dehydration. Chemical transformations occur in the hydrated paste at high temperatures leading to unhydrated compounds with cementitious characteristics. This process explains the partial recovery of strength observed in concrete structures damaged by fire when subject to post-fire curing [15]. Dehydration and decomposition reactions within the hydrated cement paste contribute to a rapid degradation of concrete properties, particularly beyond 300 °C

---

* Corresponding author. Address: Vicuña Mackenna 4860, 7820436 Macul, Chile. Tel.: +562 2 354 4244; fax: +562 2 354 4806.

E-mail addresses: rserpell@uc.cl (R. Serpell), mlopez@ing.puc.cl (M. Lopez).

0958-9465/$ - see front matter © 2013 Elsevier Ltd. All rights reserved.
http://dx.doi.org/10.1016/j.cemconcomp.2013.03.020

[16–20], as all hydrated phases of cement paste dehydrate progressively to give anhydrous phases [21], decreasing the packing density and increasing porosity of the pastes [22,23]. Upon re-saturation, rehydration of the anhydrous phases is accompanied by partial recovery of the initial pore structure and partial recovery of the mechanical properties of the paste [15,22]. However, despite the apparent reversibility, anhydrous phases obtained from dehydration are different from the anhydrous phases in the original cement. Poorly crystallized Calcium Silicate Hydrates (C–S–H) of Ca/Si ratio over 1.3 gradually decomposes over 300 °C to produce β-C_2S of high specific surface area [24]. C–S–H from hydrated cement pastes decomposes at 750 °C to form a neso-silicate similar in structure to β-C_2S, which rehydrates upon contact with ambient water producing new C–S–H [25]. This rehydration displays cementitious behavior similar to that of the calcium silicates present in Portland cement, developing strength and thus potentially enabling the production of construction materials [26].

Shui et al. [27] explored the effect of dehydration temperature between 300 °C and 900 °C over several properties of dehydrated-cement pastes such as: water requirement for standard consistency, setting time, degree of rehydration, and compressive strength. Highest 28-day compressive strength reported, equivalent to 60% of the strength developed by ordinary Portland cement pastes at the same age, was observed for pastes incorporating materials dehydrated at 800 °C. In a more recent study, the use of dehydrated-cement as an activator for fly ash in a geopolymer-like cementitious material system was investigated [28]. A design method based on the theoretical ratio of calcium to silicon was proposed, and strengths exceeding 60 MPa were achieved for steam cured pastes at 24 h.

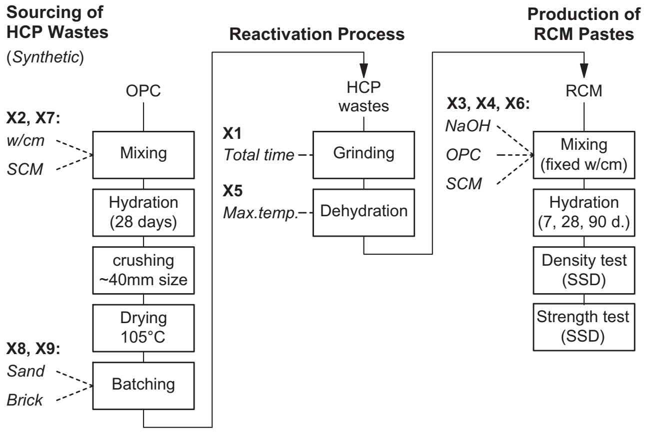

Fig. 1. Schematic diagram of experimental steps, showing factors associated with each step.

The dehydration process required to produce reactivated cementitious materials (RCMs) involves temperatures much lower than those required to produce new Portland cement, making it an interesting alternative for on-site recycling of fines derived from RCA production, or for recycling of cementitious materials from wash waters and rejected batches in concrete mixing plants. However, considering the wide variety of HCP sources which would be available, and the multiple options for both the reactivation process and the proportioning of pastes incorporating RCM, a study of the effect of a wider set of factors and factor interactions is required to evaluate this recycling alternative and to identify relevant parameters to optimize it.

In order to address these requirements, a two phase experimental study was developed beginning with an exploratory phase to identify and screen relevant factors, followed by a second phase focused on the in-depth study and characterization of their effects. This paper presents the results of a factorial experiment designed for the first phase of the study, meant to identify factors and factor interactions having a significant effect on the cementitious characteristics of the RCM as indicated by the strength development of paste specimens produced with them. A total of nine factors were selected to represent the most relevant inputs of the recycling process (Fig. 1). These factors were grouped according to their role in the process (Table 1). Factors from group I correspond to characteristics of the waste materials and account for foreseeable variations of real HCP wastes. The characteristics of the original HCP, such as its degree of hydration, composition and concentration relative to inert materials present in the wastes were expected to affect the cementitious characteristics of the RCM produced from them. In order to have control over these characteristics, cement pastes were produced under laboratory conditions to supply the HCP wastes for this study. Factors from group II correspond to parameters of the reactivation process expected to affect the cementitious characteristics of the RCM, such as the maximum temperature of the dehydration process and the fineness to which materials are grinded before dehydration. Factors from group III control the proportioning of mixtures based on RCM. In these mixtures, it was expected that free lime present in the RCM would hydrate and provide $Ca(OH)_2$ for pozzolanic reactions with SCM additions. It was also expected that inert fines present along the HCP wastes would undergo transformations during the thermal process producing materials which could benefit from the addition of an alkaline activator to the RCM-based mixtures. Finally, partial substitution of RCM by OPC in these mixtures would allow evaluation

Table 1
Assignment of experimental factors and their selected levels.

Design factors	Experimental factors		Factor group			Levels		
	Name	Description	I	II	III	−1	0	+1
X1	*FGR*	Additional grinding time (fine grinding)		o		0 min	10 min	20 min
X2	*DoH-s*	W/CM ratio of HCP waste (degree of hydration)	o			0.35	0.425	0.50
X3	*NaOH*	Alkaline activator content in RCM-paste			o	0%	3%	6%
X4	*OPC*	Portland cement replacement in RCM-paste			o	0%	2.5%	5%
X5	*T°DH*	Maximum temperature during dehydration		o		700 °C	750 °C	800 °C
X6	*SCM*	SCM replacement in RCM-paste			o	0%	5%	10%
X7	*SCM-s*	SCM replacement in HCP waste	o			0%	5%	10%
X8	*F.Si-s*	Inert siliceous fines in HCP waste (sand residues)	o			0%	5%	10%
X9	*F.Al-s*	Inert clay brick fines in HCP waste (brick residues)	o			0%	5%	10%
X10	B1	Blocking factor 1						
X11	B2	Blocking factor 2						

Notes: Factor groups indicate role of factors in the recycling process. Group I: source material factors. Group II: reactivation process factors. Group III: composition factors for RCM-based pastes.

of possible interactions between both materials for potential applications of RCM as supplementary cements.

Screening of relevant factors by identifying significant factor and factor-interaction effects provides key information for future investigations on the subject, and helps guide the characterization of HCP wastes required to select appropriate recycling processes.

2. Experimental design, materials and methods

For identification and screening purposes the design of experiments approach enables an efficient use of experimental resources and time by reducing the number of observations required to assess relative factor relevance. It provides quantitative values for the effects of factors and factor interactions enabling fitting a linear model of the response within the experimental region explored. This model can be used to determine which factors merit further attention and can be expanded later with a minimal set of additional experimental runs to develop a detailed model of the response surface, which can be used to optimize the process parameters.

2.1. Experimental design and experimental factors

A fractional factorial experimental design was selected to keep the number of experimental cases within constraints. To accommodate the nine factors under study plus two blocking factors a 2^{11-5} design was adapted from a published design [29]. This design requires only 64 experimental cases (2^6), corresponding to a 1/32th fraction (2^{-5}) of a full factorial design for 11 factors in two levels (2^{11}). The fractioning was achieved using the defining relation I =12347 =13568 =23569 = 345(10) = 126(11). This means factor X7 is mapped to the interaction of factors X1*X2*X3*X4, factor X8 is mapped to the interaction of factors X1*X3*X5*X6, factor X9 is mapped to the interaction of factors X2*X3*X5*X6, factor X10 is mapped to the interaction of factors X3*X4*X5, and factor X11 is mapped to the interaction of factors X1*X2*X6. Higher order interactions are not expected to have significant effect on the responses. However, as a consequence of fractioning some effects become aliased, i.e. some effects cannot be unambiguously estimated as they are confounded with effects of different factors or factor interactions. Nevertheless, in the selected design all main-factor effects and most of the 55 two-factor interaction effects are aliased to higher order interactions only (interactions of 3 or more factors). By careful assignment of experimental factors, most of the aliased two-factor interactions were made to involve blocking factors which are not expected to participate in interactions [30]. Only 6 two-factor interaction effects involving experimental factors remained aliased. Consequently, experimental factors least expected to display interaction effects were assigned to the design factors involved in the remaining aliased interactions.

Assignment of experimental factors to design factors is shown in Table 1 including the experimental levels selected for each factor. Factors from group I were assigned design factors X2, X7, X8 and X9. Factor X2 (*DoH-s*) corresponds to the degree of hydration of the source pastes. The water to cementitious material mass ratio (W/CM) was used as an indirect way to obtain two different levels for the degree of hydration of the source pastes at a fixed hydration time. Preliminary tests showed that the selected 0.50 and 0.35 W/CM ratios produced a significant difference in non-evaporable water content – indicative of the degree of hydration – for OPC paste samples cured under water for a fixed period of time. Factor X7 (*SCM-s*) indicates the weight substitution level of OPC by silica fume in the source paste, and is meant to test for effects due to the use of SCM in the original composition of the wastes. Factors X8 (*F.Si-s*) and X9 (*F.Al-s*) were used to assess the effect of inert fine residues of siliceous (sand) and argillaceous (clay brick) composition, respectively, which are expected to be found along HCP wastes from actual concretes. Both inert materials were incorporated as substitution by weight of source paste.

Factors from group II were assigned design factors X1 and X5. Factor X1 (*FGR*) corresponds to the fineness to which the HCP wastes are grinded prior to dehydration. The different levels of fineness were achieved extending grinding time and changing the configuration of the mill. The grinding time used for the low level of fineness resulted in 85% of the material passing the No. 200 mesh (75 μm), while the time used for the high level resulted in 85% of the material passing the No. 325 mesh (45 μm). Factor X5 (*T°DH*) corresponds to the maximum temperature reached during dehydration. Although its general effect has been characterized [27], it was included it in order to assess its potential interactions with other factors.

Factors from group III were assigned design factors X3, X4 and X6. Factor X3 (*NaOH*), indicates the addition of sodium hydroxide as an alkaline activator to the RCM mixtures. The level to which the sodium hydroxide solution was incorporated is expressed as a percentage by weight of cementitious material, but substituting the equivalent volume of mixing water, following standard practice of studies on alkali activated materials [31]. Factor X4 (*OPC*) indicates the weight substitution level of RCM by ordinary Portland cement in the mixtures. A low level of substitution was selected, as it was expected that Portland cement would outperform the corresponding amount of RCM being substituted. Finally, factor X6 (*SCM*) indicates the weight substitution level of RCM by silica fume in the mixtures.

To cope with the still large number of cases the design was divided in four blocks of 16 cases each according to the levels of the two blocking factors. Blocking factors were assigned design factors X10 and X11. Execution order of individual cases within each block was randomized. Additionally, two central cases were added in each block to enable direct estimation of the experimental variance of the response, required for the statistical significance test of the estimated effects. Central cases were executed at the average level of factors, in fixed order within each block (cases 5 and 14). For all cases in the design only one observation was performed for each response at each of the testing dates (7, 28 and 90 days). Nevertheless, due to the large number of cases in the design, the influence of potential outliers is reduced in the estimation of factor and factor interaction effects.

The main interest responses were the compressive strength of RCM-based pastes, at 7, 28 and 90 days of hydration (responses Y1, Y2 and Y3 respectively). Compressive strength was assessed on cubic specimens 20 mm in size. Additionally, the average Saturated Surface Dry (SSD) density of the specimens was measured to determine potential correlation between strength and density results.

3. Materials and methods

Source pastes to supply HCP for the reactivation process were prepared using ordinary Portland cement conforming to ASTM C150-09 type I. The SCM used was a commercially available condensed Silica fume, composed of over 99% SiO_2 according to XRF analysis. Pastes were mixed using distilled water, and cast into shallow plastic molds of 2.0 L capacity ($\sim$250 × 200 × 40 mm). As shown in Table 2, five pastes were prepared to account for the four combinations and average values of factors X2 and X7. Pastes were kept in the molds for 24 h in a fog room at 23 °C, and then unmolded and cured under water at 23 °C until 28 days of hydration. The resulting paste slabs were crushed in chunks of 40 mm maximum size which were then dried at 105 °C until constant weight to stop

Table 2
Composition of source pastes to supply HCP wastes (~2 L).

Mix	Composition				Curing (d)	Weight loss % (105 °C)
	OPC (g)	SCM	Water (g)	W/CM		
W1	2700	300 g	1050	0.35	28	17.7
W2	3000	0	1050	0.35	28	16.9
W3	2520	280 g	1400	0.50	28	25.2
W4	2800	0	1400	0.50	28	21.8
W5	2850	150 g	1275	0.425	28	21.3

hydration, and stored when still hot in sealed plastic containers to prevent hydration to proceed.

For the inert siliceous fines, Chilean standard sand (comparable to ASTM C778-06) was used. The inert clay brick fines were derived from fragments of calcined clay bricks from a local factory. These materials were proportioned according to the indicated levels of the factors for each experimental case and grinded together in batches with the corresponding amount of source HCP. Each batch totaled 150 g of material including the HCP and the indicated amount of sand (0 g or 15 g) and brick fragments (0 g or 15 g) according to the levels of factors X8 and X9 respectively. For the central cases 7.5 g of sand and 7.5 g of brick fragments were added to 135 g of HCP.

Grinding was performed in dry state, in a 600-W vibratory mill comprised of a stainless steel container where samples are placed together with a steel cylinder and a steel ring that move freely hitting the sample. All batches, including those for central cases, were grinded for an initial period of 10 min using the central cylinder only. Batches requiring higher fineness according to factor X1 were grinded for 20 additional minutes adding the ring. For the central cases the additional grinding time was 10 min. Grinded materials were stored in sealed plastic containers. Between grinding of each batch the mill was cleaned by grinding coarse sand until metal surfaces were free of residues.

Dehydration was performed in an electric muffle oven, in batches of 85 g each. The maximum dehydration temperature, indicated by factor X5, was reached at a temperature increase rate of 10 °/min starting from room temperature. Samples were kept at the maximum temperature for 1.5 h, and then left to cool down at free rate inside the oven. When the temperature inside the oven reached below 300 °C the samples were removed, weighed, and stored in sealed glass flasks while still hot.

The RCM-based pastes were mixed at 0.70 W/CM due to the high water demand of the RCM [27]. For each case a total of 35 g of cementitious material was mixed including the RCM and the indicated amount of OPC (0 g or 1.75 g) and silica fume (0 g or 3.5 g) according to the levels of factors X4 and X6 respectively. For the central cases the substituted amounts of RCM were 0.88 g by OPC and 1.75 g by silica fume. Distilled water was added at the fixed W/CM, incorporating either 0 g or 2.10 g of NaOH 8 M solution as substitution by volume of water, as indicated by the level of factor X3. For the central cases 1.05 g of NaOH 8 M solution was used. For each case a total of 59.5 g of mix was prepared, producing ~35 mL of paste. Each resulting paste was cast in three 20 mm-side cubic molds. Pastes were kept in the molds for 24 h at 23 °C in a fog room at 100% R.H. After unmolding, the cubes were cured underwater at 23 °C until the date of testing (7, 28 or 90 days).

Each cubic specimen was weighed in SSD condition to 0.01 g precision before testing. At 7 days of hydration, the cube weighing the median value of the three cubes available was selected for compressive strength testing. At 28 days the cube with the highest weight was selected, leaving the cube with the lowest weight to be tested at 90 days. Compressive strength testing was performed at a loading rate of 0.100 kN/s, equivalent to 0.25 MPa/s. Fracture was automatically detected by the testing machine and maximum load reported with 0.01 kN precision.

4. Results and discussion

Observations have no significant sign of autocorrelation which is consistent with the randomization of case execution within each block. The time order scatter plot for strength observations (Fig. 2) shows no correlation of response with execution order, and no significant location or scale shift over time despite the execution in four separated blocks. The histogram of the observations shows a bi-modal distribution spreading over a wider range of values with increasing hydration time, attributed to a factorial design in two levels in which a reduced number of factors has a strong effect on the response.

Both compressive strength and SSD density increased with hydration time in all the cases observed.

The relative strength of individual cases within each block varied significantly from 7 to 28 days of hydration. As seen in Fig. 3, a wide range of 28-day strength results was observed for cases having similar 7-day strength, making early strength a bad predictor of long term strength ($R^2 = 0.42$). Conversely, good agreement was found between 28-day and 90-day strength results ($R^2 = 0.90$), and between 7, 28 and 90-day SSD density results.

No correlation was found between SSD density and compressive strength observations at 28 days of hydration (Fig. 4). The observed variation of the compressive strength response is therefore attributed to the variation of the cementitious characteristics of the RCM produced.

Despite being produced at the average level of all experimental factors, central case specimens within each block displayed compressive strength and SSD density results significantly higher than block averages, indicating strong non-linearity of the responses in the experimental region explored. At 7 days of hydration, compressive strengths of central cases are consistently located in the upper quartile of results for each block. Although the difference is seen to

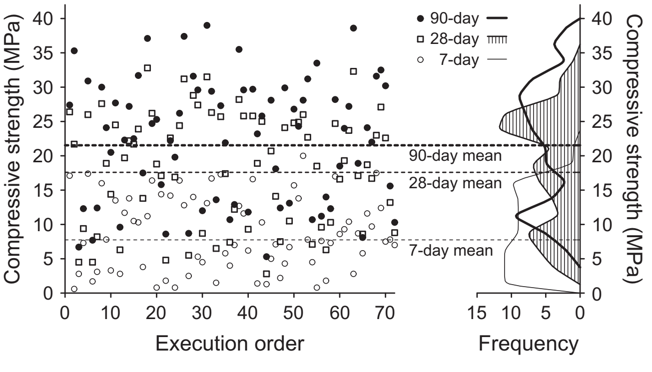

Fig. 2. Time order scatter plot of observed strength for all cases. Frequency shows bi-modal distribution of response spreading over hydration time.

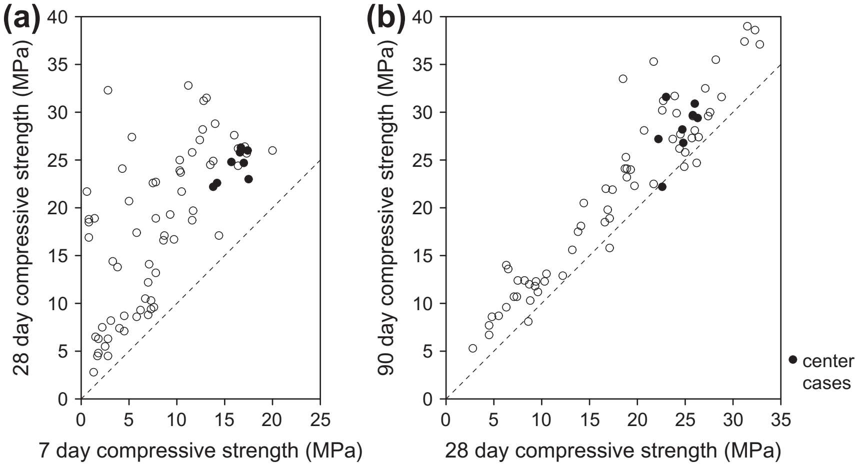

Fig. 3. Scatter plots of compressive strength observations. (a) 28-day strength versus 7-day strength and (b) 90-day strength versus 28-day strength.

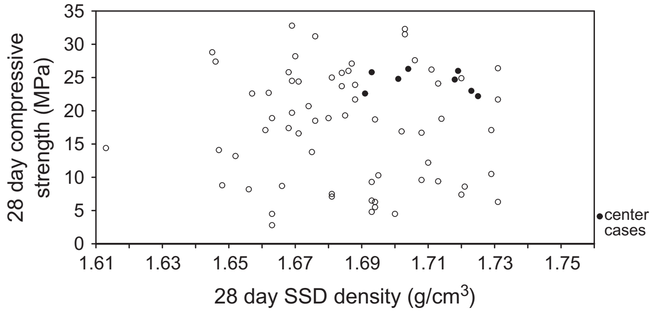

Fig. 4. Scatter plot of compressive strength observations versus SSD density observations for recycled paste specimens tested at 28 days.

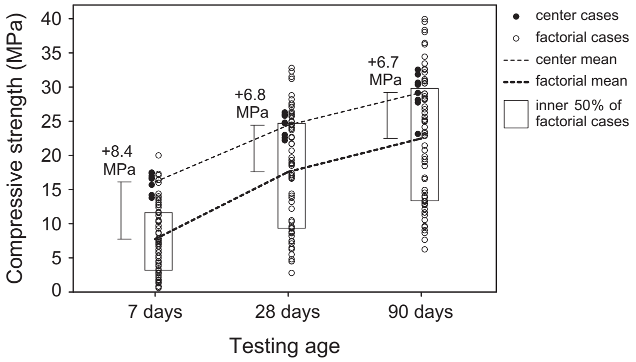

Fig. 5. Compressive strength observations at different testing ages. Average results of central cases deviate from average results of factorial cases.

decrease over time, the non-linearity is still significant at 90 days of hydration (Fig. 5).

A temperature increase was observed on the fresh paste at the moment of mixing, which is indicative of a variable amount of free lime present in the RCM. Consistency of fresh pastes also varied considerably between different cases at the fixed W/CM used. Only a subjective assessment of paste consistency was recorded during mixing, relative to which no evident correlation was found with results for compressive strength of RCM pastes.

4.1. Estimated effects of factors and factor interactions

Significance of factor and interaction effects was assessed using a statistical method complemented with a graphical method based on the normal probability plot of effects' estimates. For the statistical method, experimental variance of each response was determined from the median of the variance of the central cases within each block (4 degrees of freedom). The variance of the effects' estimates was calculated from the variance of the response considering the number of cases averaged to estimate the effects (i.e. variance of effects = 2/32 times the variance of the response). A 95% confidence interval was determined from the standard deviation of the effects' estimates and the corresponding points of the t distribution for a 5% probability with 4 degrees of freedom (Table 3).

The estimates for effects of factors and two-factor interactions on compressive strength of RCM-based pastes at 7, 28, and 90 days of hydration are shown in Tables 4–6 respectively. Effects exceeding the 95% confidence interval criteria are marked in bold typeface. Estimates for aliased effects are marked in italic typeface. All reported values are in units of the response, i.e. MPa. A relevance index is proposed for each factor, calculated as the ratio of the sum of the magnitude of its significant effects only, over the average maximum range of the response. If the main and interaction effects of a single factor could explain all the observed range of the response its relevance index would be close to one.

4.2. Identification of significant factor and factor-interaction effects

Half-normal probability plots of the 63 effects of factors and factor interactions which can be estimated using the selected experimental design display good overall agreement between the selected 95% confidence interval and the graphical assessment of significance of effects. In these plots significant effects are expected to deviate from the line representing a normal distribution of effect estimates, meaning they cannot be explained by random errors. In the half normal plot of effects on 7-day compressive strength

Table 3
Variance $\left(S_R^2\right)$ and standard deviation (S_R) of responses and effects (S_{Ef}).

	Compressive strength		
	Y1 (7 days)	Y2 (28 days)	Y3 (90 days)
$\left(S_R^2\right)$	1.83 (4 DoF)	4.12 (4 DoF)	6.31 (4 DoF)
S_R	1.35 MPa	2.03 MPa	2.51 MPa
S_{Ef}	0.34 MPa	0.51 MPa	0.63 MPa
95% C.I. effects	±0.94 MPa	±1.41 MPa	±1.74 MPa

Table 4
Effect of factors and interactions over response Y1: 7-day compressive strength of RCM pastes (MPa). 95% confidence interval = ±0.94 MPa.

Factor		Main effects	Two-factor interaction effects								Relevance[*]
			X2 *DoH-s*	X3 *NaOH*	X4 *OPC*	X5 *T°DH*	X6 *SCM*	X7 *SCM-s*	X8 *F.Si-s*	X9 *F.Al-s*	
X1	*FGR*	−0.68	***−1.23***	**1.69**	−0.05	**−1.36**	**−1.23**	**3.36**	*0.05*	*0.55*	**0.53**
X2	*DoH-s*	**2.46**		0.13	0.20	0.01	0.36	**1.12**	*0.55*	*0.05*	**0.29**
X3	*NaOH*	**1.86**			−0.91	**2.15**	**2.01**	**1.24**	−0.36	0.18	**0.53**
X4	*OPC*	0.05				0.40	−0.41	−0.44	−0.37	0.15	0.00
X5	*T°DH*	**−1.55**					**−1.04**	**−3.07**	0.31	−0.07	**0.55**
X6	*SCM*	**4.76**						−0.05	0.86	−0.36	**0.54**
X7	*SCM-s*	**1.77**							−0.05	**−1.30**	**0.71**
X8	*F.Si-s*	**−1.70**								***−1.23***	0.18
X9	*F.Al-s*	**−1.11**									0.14

[*] Sum of absolute values of significant effects of factor compared to maximum range of response.

Table 5
Effect of factors and interactions over response Y2: 28-day compressive strength of RCM pastes (MPa). 95% confidence interval = ±1.41 MPa.

Factor		Main effects	Two-factor interaction effects								Relevance[*]
			X2 *DoH-s*	X3 *NaOH*	X4 *OPC*	X5 *T°DH*	X6 *SCM*	X7 *SCM-s*	X8 *F.Si-s*	X9 *F.Al-s*	
X1	*FGR*	0.35	*−1.13*	**1.51**	−0.45	−1.22	−0.13	**3.61**	*1.12*	*1.37*	**0.19**
X2	*DoH-s*	**3.04**		−0.10	−0.56	0.68	0.61	**1.53**	*1.37*	*1.12*	**0.17**
X3	*NaOH*	**−5.16**			**−1.45**	−0.10	**1.49**	−1.38	0.69	0.60	**0.36**
X4	*OPC*	−0.14				−0.02	−1.08	−0.65	0.47	0.58	0.06
X5	*T°DH*	**2.65**					−0.95	**−1.50**	0.29	−0.25	**0.16**
X6	*SCM*	**12.37**						−1.10	1.25	−0.30	**0.52**
X7	*SCM-s*	**3.85**							0.17	**−2.02**	**0.47**
X8	*F.Si-s*	**−2.50**								*−1.13*	0.09
X9	*F.Al-s*	−1.18									0.08

[*] Sum of absolute values of significant effects of factor compared to maximum range of response.

Table 6
Effect of factors and interactions over response Y3: 90-day compressive strength of RCM pastes (MPa). 95% confidence interval = ±1.74 MPa.

Factor		Main effects	Two-factor interactions								Relevance[*]
			X2 *DoH-s*	X3 *NaOH*	X4 *OPC*	X5 *T°DH*	X6 *SCM*	X7 *SCM-s*	X8 *F.Si-s*	X9 *F.Al-s*	
X1	*FGR*	0.93	*−0.89*	1.58	0.63	−1.60	0.12	**2.87**	*0.73*	*0.68*	**0.09**
X2	*DoH-s*	**2.17**		0.05	−1.07	−0.08	0.65	0.34	*0.68*	*0.73*	0.07
X3	*NaOH*	**−8.50**			−1.23	−1.45	0.23	−1.56	0.57	0.20	**0.28**
X4	*OPC*	−0.07				−0.52	−0.74	−0.55	0.17	1.01	0.00
X5	*T°DH*	**2.83**					−0.62	−0.20	0.83	−0.02	**0.09**
X6	*SCM*	**13.85**						−0.56	**2.04**	−0.14	**0.52**
X7	*SCM-s*	**3.92**							0.30	−0.89	**0.22**
X8	*F.Si-s*	**−2.16**								*−0.89*	**0.14**
X9	*F.Al-s*	−0.27									0.00

[*] Sum of absolute values of significant effects of factor compared to maximum range of response.

(Fig. 6), several effects exceeding the selected confidence interval lay on the normal distribution line and thus they were screened out. Consequently, 6 factors and five two-factor interactions were identified as having a significant effect on 7-day strength of RCM-based pastes.

In the half-normal probability plot of effects on 28-day compressive strength (Fig. 7) it is evident that several effects just exceeding the selected confidence interval lay on the normal distribution line and thus they were screened out. Consequently, a total of 6 factors and 2 two-factor interactions were identified as having a significant effect on 28-day strength of RCM-based pastes. Several of these factors and interactions also have a significant effect on 7-day strength; however, their relative importance differs substantially between the two testing ages.

Conversely, in the half normal plot of effects on 90-day compressive strength (Fig. 8), several estimated effects not exceeding the selected confidence interval deviate from the normal distribution line and thus they were included in the analysis of effects. The set of factors and interactions considered is similar to the corresponding set of factors and interactions having a significant effect on 28-day compressive strength, with minor differences in the relative importance of their effects. Consequently, a total of 6 factors and 6 two-factor interactions were identified as having a significant effect on 90-day compressive strength of RCM-based pastes.

Considering all hydration ages, a total of 6 factors and 9 two-factor interactions were identified as having a significant effect on compressive strength of the RCM-based pastes. Factors due to characteristics of HCP wastes displaying significant main effects were: the degree of hydration of the HCP wastes (X2), the use of silica fume in the composition of the HCP (X7) and the presence of inert siliceous fines intermixed in the HCP wastes (X8). Factor X7 was also involved in 4 significant two-factor interaction effects. Among reactivation process factors temperature of dehydration (X5) displayed a significant main effect, while the fineness of the

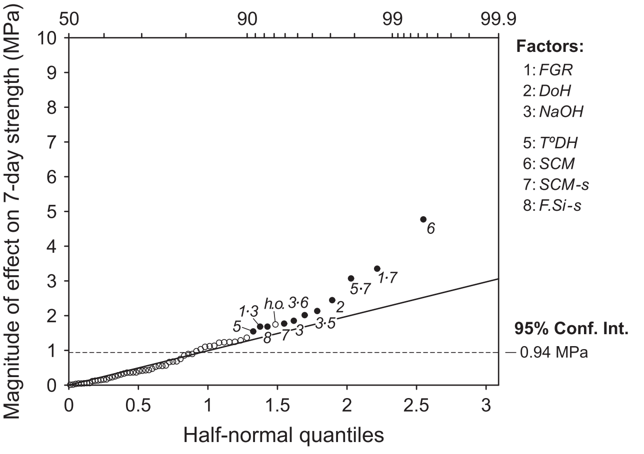

Fig. 6. Half-normal probability plot of estimated effects on 7-day compressive strength (h.o.: higher order effect, not considered).

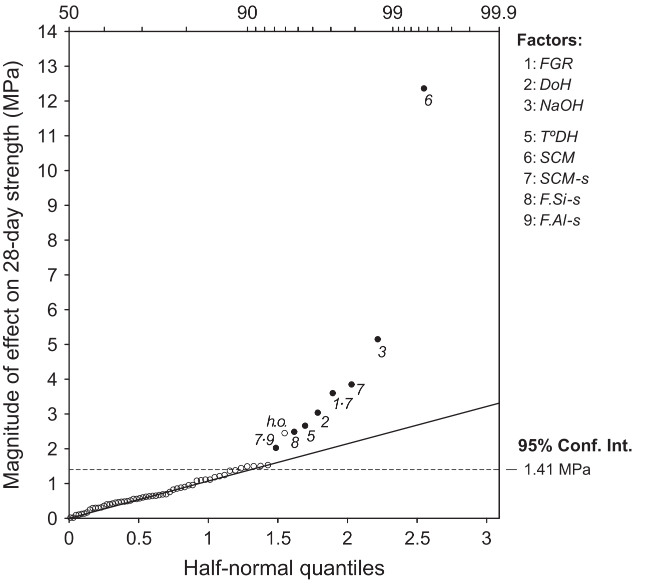

Fig. 7. Half-normal probability plot of estimated effects on 28-day compressive strength (h.o.: higher order effect, not considered).

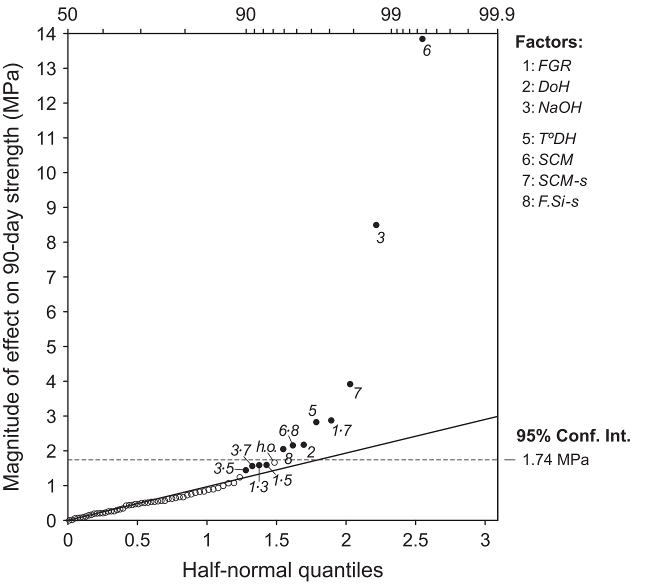

Fig. 8. Half-normal probability plot of estimated effects on 90-day compressive strength (h.o.: higher order effect, not considered).

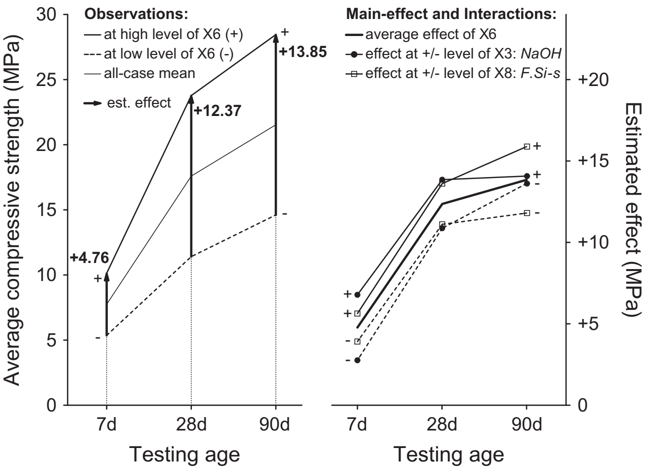

Fig. 9. Average compressive strength of RCM-based pastes at different levels of substitution of RCM by silica fume in the mixtures (factor X6), showing factor and interaction effects.

wastes (X1) was involved only in significant two-factor interaction effects. Factors due to the proportioning of RCM-based pastes displaying significant main effects were: the addition of sodium hydroxide to the RCM-based pastes (X3) and the substitution of RCM by silica fume (X6), with both factors involved in several significant two-factor interaction effects.

4.3. Analysis of estimated effects on compressive strength of RCM-based pastes

Compressive strength of RCM-based pastes was most affected by the level of substitution of RCM by silica fume (factor X6). In the experimental region explored, increasing the level of silica fume substitution in the RCM-based mixtures from 0% to 10% significantly increases average strength of the resulting pastes at all ages tested (Fig. 9). This indicates RCM have a significant capacity for activating pozzolanic reactions. In addition, the estimated effect of silica fume substitution is higher when 5% NaOH solution is added to the RCM-based mixtures (interaction X6·X3). This interaction effect decreases gradually, being insignificant at 90 days. A possible explanation might be that the addition of NaOH solution potentiates the reactions involving silica fume in the RCM-based pastes at early ages, as OH^- ions promote the dissolution of the amorphous silica. Similarly, the effect of silica fume substitution is higher when the HCP wastes contain 10% inert siliceous fines (interaction X6·X8). At 90 days of hydration this interaction effect is of similar magnitude than the negative effect of the inert siliceous fines on strength.

The effect of NaOH addition to the RCM-based mixtures (factor X3) was seen to evolve over hydration time. In the experimental region explored, increasing the addition of NaOH solution from 0% to 5% increases average strength of the resulting pastes at 7 days but decreases it at 28 and 90 days (Fig. 10). Similar behavior has been observed in OPC-based and C_3S-based pastes incorporating NaOH solutions. A reduced induction period and a general acceleration of initial hydration reactions are reported, however resulting in lower long term strength, probably due to replacement of Ca^{2+} ions by Na^+ affecting the microstructure of the formed C–S–H [32]. The effect of the NaOH addition is affected by the level of

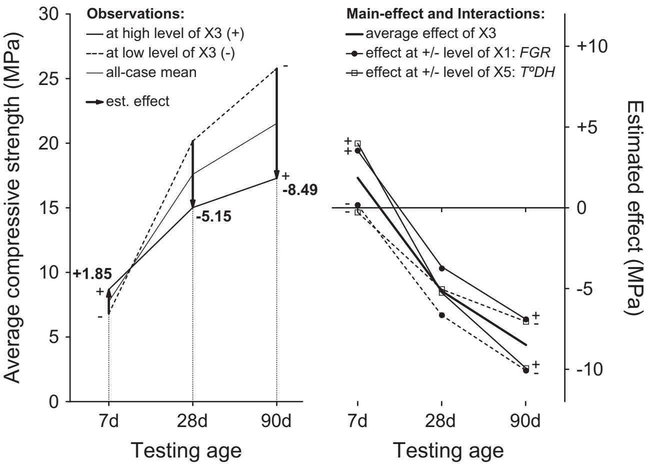

Fig. 10. Average compressive strength of RCM-based pastes at different levels of incorporation of NaOH solution to the mixtures (factor X3), showing factor and interaction effects.

grinding of the HCP wastes (interaction X3·X1) and by the dehydration temperature used in the reactivation process (interaction X3·X5). When the HCP are grinded to higher fineness, the estimated effect of the NaOH addition is higher at 7 days, but lower at 28 and 90 days. This interaction increases the positive effect of NaOH on 7-day strength and decreases its negative effect at later ages. When HCP wastes are dehydrated at 800 °C, the estimated effect of the NaOH addition is higher at 7 and 90 days, increasing its positive effect on early strength, however, also increasing its negative effect on long term strength. It is suspected that both interactions are related to the availability of Ca^{2+} ions affecting the activity of Na^{+} ions in the RCM-based mixtures [33]. Extended grinding process can result in extended carbonation of calcium bearing compounds, decreasing the availability of calcium ions in solution due to the low solubility of $CaCO_3$. Conversely, a higher dehydration temperature involves more decomposition of calcium bearing compounds into CaO, which readily combines with water to form soluble $Ca(OH)_2$, increasing the availability of Ca^{2+} ions.

Presence of silica fume substituting OPC in the original composition of the HCP wastes (factor X7) had a positive effect on compressive strength. In the experimental region explored, increasing the level of silica fume substitution in the source HCP from 0% to 10% increases average strength of RCM-based pastes (Fig. 11). This is consistent with the product from C–S–H dehydration having a significant role in the strength gain of the RCM-based pastes, assuming more C–S–H should have formed as a product of pozzolanic reactions in the HCP incorporating silica fume. The estimated effect of silica fume substitution in the source HCP is higher when the HCP wastes are grinded to higher fineness (interaction X7·X1). It is believed that through extended grinding a significant amount of unreacted silica fume from the HCP wastes becomes available for pozzolanic reactions in the RCM-based pastes, increasing strength in agreement with the estimated effect of factor X6. Conversely, when the HCP are dehydrated at 800 °C the estimated effect of the silica fume substitution in the source HCP is lower at 7 and 28 days (interaction X7·X5). Likewise, the estimated effect of the silica fume substitution in the source HCP is lower at all ages tested when the HCP contain 10% inert fines from clay bricks (interaction X7·X9). It must be noted that the combined effect of the three interactions involving this factor can increase or decrease its effect by more than 7 MPa at 7 and 28 days, when the other factors involved are set at the appropriate levels.

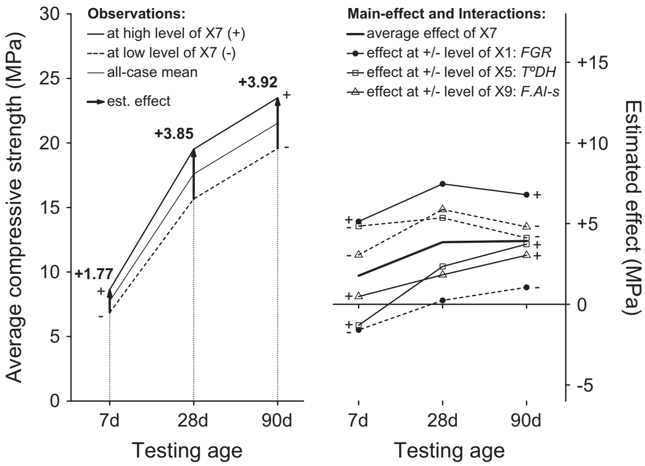

Fig. 11. Average compressive strength of RCM-based pastes at different levels of presence of silica fume in original composition of HCP wastes (factor X7), showing factor and interaction effects.

The effect of the dehydration temperature during the reactivation process (factor X5) was seen to evolve over time. In the experimental region explored, increasing the dehydration temperature from 700 °C to 800 °C decreases average strength of the RCM-based pastes at 7 days, but increases it at 28 and 90 days (Fig. 12). A varying proportion of different dehydrated products in the RCM, resulting from the different dehydration temperatures used, could be the cause of the observed effect. The estimated effect of the dehydration temperature depends on the extent of grinding of the HCP wastes (interaction X5·X1), being higher when the HCP wastes are grinded to higher fineness.

Remaining significant main-factor effects are shown in Fig. 13. In the experimental region explored, increasing the W/CM ratio of the source HCP from 0.35 to 0.50, i.e. increasing the degree of hydration of the HCP (factor X2), increases average strength of RCM-based pastes at all ages tested. A higher degree of hydration involves more C–S–H available for reactivation. However, the higher degree of hydration also means less unreacted cement remaining in the HCP wastes. Nevertheless, the calcium silicate produced from the dehydration of C–S–H probably has a high surface area, and could be more active during rehydration than the remaining unreacted cement grains which are usually concealed under a layer of dense hydration products. Finally, in the experimental region explored, increasing the content of inert siliceous fines in the HCP (factor X8) from 0% to 10% decreases average strength of RCM-based pastes at all ages tested.

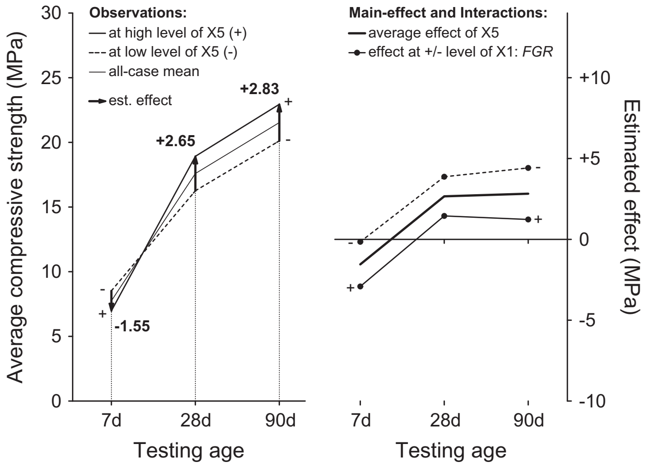

Fig. 12. Average compressive strength of RCM-based pastes at different levels of dehydration temperature (factor X5), showing factor and interaction effects.

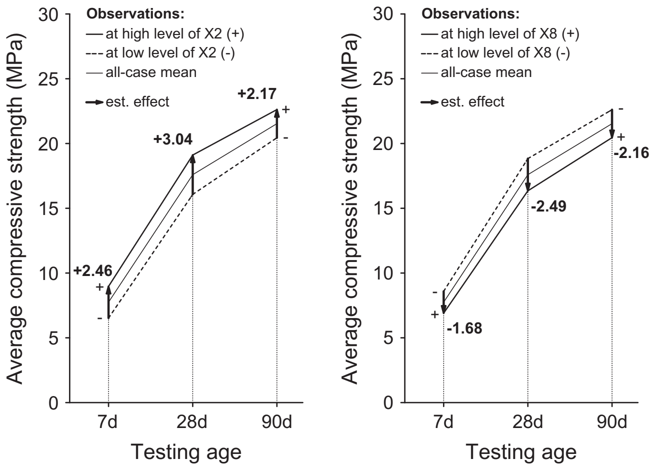

Fig. 13. Average compressive strength of RCM-based pastes at different levels of degree of hydration of HCP wastes (factor X2) and at different levels of presence of inert siliceous fines along the HCP wastes (factor X8).

4.4. Response models

The factorial experimental design performed allows for the fitting of a linear model of the response based on the estimated effects of factors and interactions. Although results from central cases indicate the response is strongly non-linear in the experimental region explored, the source of this non-linearity cannot be identified from the experiment as designed and performed. Consequently, the models reported were fitted to the factorial experimental cases only. These models are meant solely to confirm the selection of significant factors according to the screening and identification purposes of the study, and, therefore, they include only the non-confounded main-factor and two-factor interaction effects identified as significant. Models for compressive strength of recycled pastes at 7, 28, and 90 days, are respectively:

$$\begin{aligned} Y_{i1} = 7.73 &+ 1.23X_{i2} + 0.93X_{i3} - 0.77X_{i5} + 2.38X_{i6} + 0.89X_{i7} \\ &- 0.85X_{i8} + 0.85X_{i1}X_{i3} - 0.68X_{i1}X_{i5} + 1.68X_{i1}X_{i7} \\ &+ 1.07X_{i3}X_{i5} + 1.01X_{i3}X_{i6} - 1.53X_{i5}X_{i7} + \varepsilon_{i1} \end{aligned} \tag{1}$$

$$\begin{aligned} Y_{i2} = 17.57 &+ 1.52X_{i2} - 2.58X_{i3} + 1.33X_{i5} + 6.18X_{i6} \\ &+ 1.92X_{i7} - 1.25X_{i8} + 1.81X_{i1}X_{i7} - 1.01X_{i7}X_{i9} + \varepsilon_{i2} \end{aligned} \tag{2}$$

$$\begin{aligned} Y_{i3} = 21.51 &+ 1.08X_{i2} - 4.25X_{i3} + 1.41X_{i5} + 6.92X_{i6} + 1.96X_{i7} \\ &- 1.08X_{i8} + 0.79X_{i1}X_{i3} - 0.80X_{i1}X_{i5} + 1.44X_{i1}X_{i7} \\ &- 0.72X_{i3}X_{i5} + 0.78X_{i3}X_{i7} + 1.02X_{i6}X_{i8} + \varepsilon_{i3} \end{aligned} \tag{3}$$

where for any particular observation i, Y_{iz} is the predicted response, X_{ij} is the coded level of every X_j factor (−1, +1), and ε_{iz} is the random error of the respective response. In these equations the regression coefficients are in response units (MPa). As seen in Fig. 14, the models fit the experimental data and display approximately normal distributions for the residuals. The model for the compressive strength at 90 days displays the least amount of deviation from the observed values, with the lowest standard error of the estimate (2.20 MPa). This error compares well with the standard deviation of the response calculated from the central case results at 90 days (2.51 MPa). The model for compressive strength at 28 days, which includes the least number of effects, displays the largest deviation from the observed values. The model for 7-day compressive

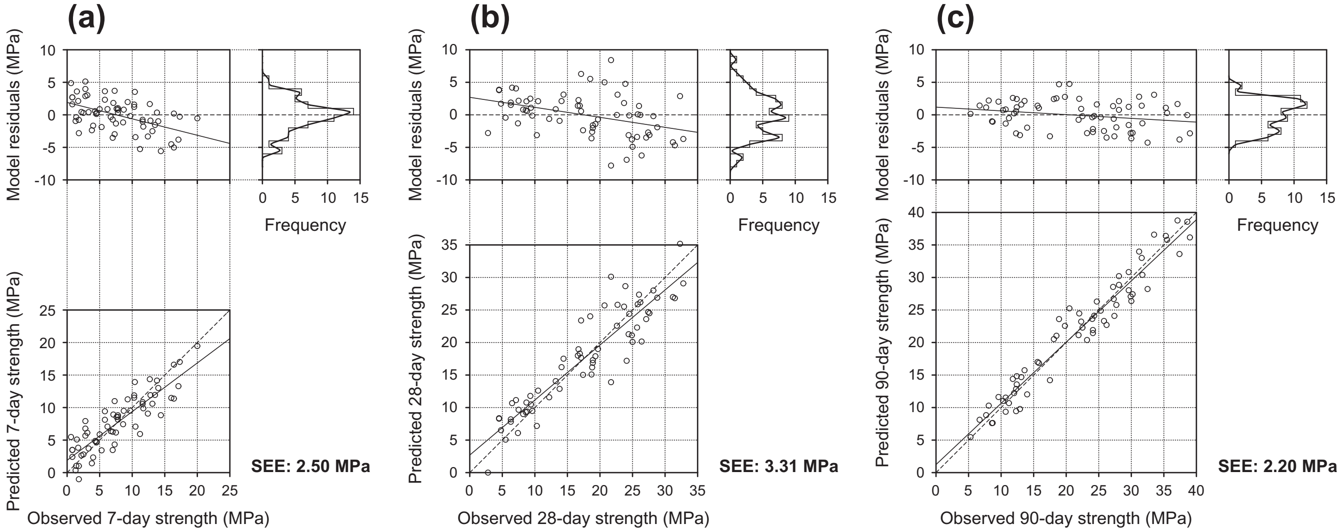

Fig. 14. Scatter plots of predicted (model) versus observed compressive strength at 7, 28, and 90 days, including residual versus observed values, and histogram of residuals.

Table 7
Combinations of factor levels for optimum long term strength.

Conditions	Factors (coded levels)									Responses			
	HCP waste composition				Reactivation		RCM-paste mixture			Strength			Density
	X2	X7	X8	X9	X1	X5	X3	X4	X6	(MPa)			(g/cm^3)
	DoH-s	*SCM-s*	*F.Si-s*	*F.Al-s*	*FGR*	*T°DH*	*NaOH*	*OPC*	*SCM*	7-d	28-d	90-d	28-d
a	+	–	+	+	–	+	–	–	+	10.6	28.8	36.1	1.686
b	+	+	+	+	+	+	–	–	+	6.2	30.7	38.4	1.686
c	+	+	+	+	–	–	–	–	+	11.3	24.4	32.9	1.643
d	+	–	–	–	–	+	–	–	+	12.3	29.3	36.3	1.708

strength displays normally distributed residuals, however with a marked drift towards under estimation of the response for higher strength observations. The general fit of the models indicates a substantial portion of the range of strength results is explained by the effect of the selected factors and interactions. Additionally, the selection of factors is confirmed to be particularly adequate to explain and predict long term strength response.

4.5. Optimum levels of factors

Within the experimental region explored the models can be used to predict combinations of factor levels yielding highest strength. Since the effect of factors and interactions evolve over time, there is not a particular combination of factors that can maximize early and long term strength simultaneously. Considering 90-day strength of RCM-based pastes as the most relevant response, optimal levels of factors for four different initial conditions (a, b, c and d) are given in Table 7. In all cases higher strength of RCM-based paste would be obtained at a high level of substitution of RCM by silica fume. For HCP wastes including inert fines from either sand or brick residues (condition a), highest long term strength of RCM-based pastes would be obtained if wastes have a high degree of hydration, and reactivating them at the higher temperature of dehydration. However, for HCP wastes including silica fume (condition b), the highest strength would be obtained increasing the time of grinding of the wastes.

If grinding time and temperature of dehydration are set at their low levels less energy would be required for the reactivation process (condition c). In this scenario, higher strengths would be obtained from HCP wastes including silica fume and having a high degree of hydration. An additional waste beneficiation process might be implemented, incorporating a silica-rich SCM and improving hydration of the wastes, for instance by wet grinding of the wastes. Finally, for HCP wastes from pure pastes (condition d) the highest strengths would be obtained for HCP having a high degree of hydration, reactivating them at the higher dehydration temperature.

5. Conclusions

In order to evaluate a thermal reactivation process as an alternative for the recycling of hydrated cement paste (HCP) wastes, it was first necessary to identify factors affecting the performance of the reactivated cementitious material (RCM) obtained. This study has contributed to our knowledge of the reactivation process and its products by screening relevant material and process factors, identifying their main effects and interaction effects on compressive strength of RCM-based pastes.

RCM display significant cementitious behavior as indicated by the strength gain of pastes made with them at 0.7 W/CM ratio. Maximum individual case values were: 20.0 (±1.4), 32.8 (±2.0), and 39.0 (±2.5) MPa at 7, 28, and 90 days, respectively. However, these maximum values were observed at different combinations of factor levels at the different testing ages. Therefore, the effects of factors on compressive strength evolve over time. This is particularly evident between 7 and 28 days of hydration. Since no correlation was found between strength and density results, differences in strength among individual cases are likely explained by the different cementitious characteristics of the RCM produced at the different levels of the factors.

Average strength of central cases, i.e. those performed at the medium level of the factors, was significantly higher than the average strength of the rest of the cases in the experiment. This indicates a large non-linearity of the response in the experimental region explored. However, identification of factors causing the reported non-linearity is beyond the possibilities of the selected factorial experimental design in two levels.

Effects of factors were estimated by linear regression of the results of the experimental design. Significance of estimated effects was determined by comparing their magnitude with the standard deviation of the effects, with a 95% confidence interval, and by a graphical method. Considering results from the three testing ages covered, 6 main-factor and 9 two-factor interactions, involving 7 of the factors under study, were identified as having a significant effect on strength of RCM-based pastes.

In the experimental region explored:

1. Increasing RCM substitution by silica fume as SCM in RCM-based pastes significantly increases their average strength, indicating RCM have substantial pozzolanic activation capacity. Additionally, this effect is higher for RCM produced from HCP wastes containing inert siliceous fines.
2. Increasing addition of NaOH alkaline activator in RCM-based pastes increases their early age strength, but decreases their long term strength. Although the activator is involved in several significant interactions, the combined effect of the factor and its interactions did not prove beneficial for the strength of RCM-based pastes.
3. Increasing the degree of hydration of the HCP wastes increases average strength of RCM-based pastes. At a high degree of hydration HCP is expected to contain a higher concentration of C–S–H. Therefore, the dehydrated product of C–S–H is regarded as a significant cementitious component of RCM.
4. Increasing substitution of OPC by silica fume in the source HCP increases average strength of RCM-based pastes. This effect increases significantly when the wastes are grinded to higher fineness. Conversely, it decreases when the wastes are dehydrated at the higher temperature or when the wastes contain fines from clay bricks.
5. Increasing the dehydration temperature used to reactivate the HCP wastes decreases average early strength of RCM-pastes, but significantly increases their long term strength. However, the effect of dehydration temperature is shifted up when the wastes are grinded to a lower fineness, rendering the negative effect on early strength insignificant.
6. Increasing the content of inert fines in the HCP wastes decreases the average strength of RCM-based pastes due to dilution of the cementitious material. However, this negative effect is significant only for the fines from siliceous sand. In the range of substitution levels studied, the effect of fines from clay bricks is hardly detectable at 90 days of hydration, suggesting these fines are better incorporated in the hydration products responsible for strength gain.

Based on the number of their significant factor and factor interaction effects the following factors have the highest potential for optimization of strength of RCM-based pastes:

Source material factors (group I):
  Degree of hydration of the HCP wastes.
  Use of silica fume in the original composition of the HCP.
  Presence of inert siliceous fines along the HCP wastes.

Reactivation process factors (group II):
  Extent of grinding of the HCP wastes.
  Maximum dehydration temperature.

Proportioning factors for RCM-based mixtures (group III):
  Substitution of RCM by silica fume.

Besides the exploration of the selected factors through a wider set of levels and on a wider set of interest responses, a better understanding of the physical and chemical processes explaining the estimated effects would be required to implement this recycling alternative for HCP wastes from concretes. Developing of alternative or additional process steps and optimization of the reactivation process to accommodate the relevant characteristics of real wastes will undoubtedly follow. However, the great potential of these materials has been established.

Acknowledgement

The authors wish to thank the "Laboratorio de Resistencia de Materiales, RESMAT (DICTUC)" for its collaboration, and Mr. Mauricio Guerra of the Construction Materials Laboratory of the School of Engineering at Pontificia Universidad Católica de Chile for his work to support this study.

References

[1] US Geological Survey. Cement statistics and information. In: Mineral Commodity Summaries. US Geological Survey. US Department of the Interior. Reston. 2009. p. 40–1. <http://minerals.usgs.gov/minerals/pubs/commodity/cement/index.html> [2009-11-18].

[2] Huntzinger DN, Eatmon TD. A life-cycle assessment of Portland cement manufacturing: comparing the traditional process with alternative technologies. J Clean Prod 2009;17:668–75.

[3] Meyer C. The greening of the concrete industry. Cem Concr Compos 2009;31:601–5.

[4] Gartner E. Industrially interesting approaches to "low-CO_2" cements. Cem Concr Res 2004;34:1489–98.

[5] Juenger MCG, Winnefeld F, Provis JL, Ideker JH. Advances in alternative cementitious binders. Cem Concr Res, in press. http://dx.doi.org/10.1016/j.cemconres.2010.11.012.

[6] Lauritzen EK. Recycling concrete – an overview of challenges and opportunities. In: Liu TC, Meyer C, editors. Recycling concrete and other materials for sustainable development. Farmington Hills: American Concrete Institute; 2004. p. 1–10.

[7] Abbas A, Fathifazl G, Isgor OB, Razaqpur AG, Fournier B, Foo S. Durability of recycled aggregate concrete designed with equivalent mortar volume method. Cem Concr Compos 2009;31(8):555–63.

[8] Lin Y, Tyan Y, Chang T, Chang C. An assessment of optimal mixture for concrete made with recycled concrete aggregates. Cem Concr Res 2004;34:1373–80.

[9] Poon CS, Shui ZH, Lam L. Effect of microstructure of ITZ on compressive strength of concrete prepared with recycled aggregates. Constr Build Mater 2004;18:461–8.

[10] Kasai Y. Recent trends in recycling of concrete waste and use of recycled aggregate concrete in Japan. In: Liu TC, Meyer C, editors. SP219-Recycling concrete and other materials for sustainable development. Farmington Hills: American Concrete Institute International; 2004. p. 11–34.

[11] Poon C, Qiao XC, Chan D. The cause and influence of self-cementing properties of fine recycled concrete aggregates on the properties of unbound sub-base. Waste Manage 2006;26:1166–72.

[12] Achtemichuk S, Hubbard J, Sluce R, Shehata MH. The utilization of recycled concrete aggregate to produce controlled low-strength materials without using Portland cement. Cem Concr Compos 2009;31:564–9.

[13] Fridrichová M. Hydration of belite cements prepared from recycled concrete residues. Ceram Silik 2007;51:45–51.

[14] Ai H, Wei J, Bai J, Lu P. Properties of recycled-cement produced from waste concrete. Adv Eng Mater 2011;194–196:1170–5.

[15] Poon CS, Azhar S, Anson M, Wong Y. Strength and durability recovery of fire-damaged concrete after post-fire-curing. Cem Concr Res 2001;31:1307–18.

[16] Phan L, Lawson J, Davis F. Effects of elevated temperature exposure on heating characteristics, spalling, and residual properties of high performance concrete. Mater Struct 2001;34:83–91.

[17] Handoo SK, Agarwal S, Agarwal SK. Physicochemical, mineralogical, and morphological characteristics of concrete exposed to elevated temperatures. Cem Concr Res 2002;32:1009–18.

[18] Janotka I, Mojumdar SC. Thermal analysis at the evaluation of concrete damage by high temperatures. Therm Anal Cal 2005;81:197–203.

[19] Arioz O. Effects of elevated temperatures on properties of concrete. Fire Saf J 2007;42:516–22.

[20] Mendes A, Sanjayan J, Collins F. Phase transformations and mechanical strength of OPC/Slag pastes submitted to high temperatures. Mater Struct 2008;48:345–50.

[21] Castellote M, Alonso C, Andrade C, Turrillas X, Campo J. Composition and microstructural changes of cement pastes upon heating, as studied by neutron diffraction. Cem Concr Res 2004;34:1633–44.

[22] Farage MCR, Sercombe J, Gallé C. Rehydration and microstructure of cement paste after heating at temperatures up to 300 °C. Cem Concr Res 2003;33:1047–56.

[23] DeJong MJ, Ulm F. The nanogranular behavior of C–S–H at elevated temperatures (up to 700 °C). Cem Concr Res 2007;37:1–12.

[24] Okada Y, Sasaki K, Zhong B, Ishida H, Mitsuda T. Formation processes of B-C2S by the decomposition of hydrothermally prepared C–S–H with $Ca(OH)_2$. J Am Ceram Soc 1994;77:1319–23.

[25] Alonso C, Fernandez L. Dehydration and rehydration processes of cement paste exposed to high temperature environments. J Mater Sci 2004;39:3015–24.

[26] Shui Z, Xuan D, Wan H, Cao B. Rehydration reactivity of recycled mortar from concrete waste experienced to thermal treatment. Constr Build Mater 2008;22:1723–9.

[27] Shui Z, Xuan D, Chen W, Yu R, Zhang R. Cementitious characteristics of hydrated cement paste subjected to various dehydration temperatures. Constr Build Mater 2009;23:531–7.

[28] Shui Z, Yu R, Dong J. Activation of fly ash with dehydrated cement paste. ACI Mater J 2011;108:204–8.

[29] NIST/SEMATECH. e-Handbook of Statistical Methods. National Institute of Standards and Technology NIST; 2003.

[30] G.E.P. Box, J.S. Hunter, W.G. Hunter. Statistics for Experimenters. 2nd Ed. John Wiley & Sons. Inc. Hoboken. New Jersey. 2005. Page 212.

[31] Dombrowski K, Buchwald A, Weil M. The influence of calcium content on the structure and thermal performance of fly ash based geopolymers. J Mater Sci 2007;42:3033–43.

[32] Juenger MCG, Jennings HM. Effects of High Alkalinity on Cement Pastes. ACI Mater J 2001;98:251–5.

[33] Peterson VK, Neumann DA, Livingston RA. Effect of NaOH on the kinetics of tricalcium silicate hydration: a quasielastic neutron scattering study. Chem Phys Lett 2006;419:16–20.